06515-5-T

Copy No. ____

THE UNIVERSITY OF MICHIGAN

COLLEGE OF ENGINEERING

DEPARTMENT OF ELECTRICAL ENGINEERING

Radiation Laboratory

STUDY OF PROBLEM AREAS IN OPTICAL COMMUNICATIONS

Interim Report No. 5

6515-5-T = RL-2141

1 April through 30 June 1965

Contract No. AF 33(615)-1021
Proj. 4335 Task 433511
Contract Monitor, Mr. Frank Polak AVWC

G. Hok, M. L. Barasch, P. Lambropoulos and E. K. Miller

31 July 1965

Incomplete - some pages used for Final

Contract With: Air Force Avionics Laboratory, AVWC
Research and Technology Division, AFSC
Wright-Patterson AFB, Ohio 45433

Administered through:
OFFICE OF RESEARCH ADMINISTRATION • ANN ARBOR

TABLE OF CONTENTS

LIST OF FIGURES

ABSTRACT

Graphs of slant-path transmittance versus wavenumber from various altitudes are presented and discussed.

The relation between the channel capacity and bandwidth of an optical channel is considered, and an upper bound for the practically useful bandwith is suggested. The statistical theory of detection of coherent signals against a background of thermal radiation is further discussed on the basis of results derived in the previous report. Numerical calculations of some statistical characteristics under various conditions are given in graphical form. Similarities and differences in comparison with a classical communication channel are discussed.

Error-reducing codes for binary asymmetric channels may be designed on the basis of the permutation principle of Slepian. The analogy between the redundancy structure of these codes and that of parity codes suggests extensions to higher-order error-correcting codes. The design of such codes for channels with extremely high error rate does not appear promising.

The bandpass-filter properties of a laser amplifier is studied theoretically; the nonzero width of the energy levels of the active material is introduced by means of damping theory.

I. INTRODUCTION

The three problem areas recommended for investigation under this project were outlined in the introduction to the First Interim Report (Barasch et al,1964). Detailed presentations of research carried out in these areas have been included in the Interim Reports Nrs. 2-4 (Hok et al, 1964, January 1965, April 1965). Work in one problem area concerned with narrow-band, preferably tunable optical filters, was terminated with the presentation of the Second Interim Report.

A second chapter of this report presents material in the first problem area, which concerns propagation, scattering and absorption of visible and infrared radiation between deep space and points on the earth. From tables available in the recent literature data is presented in graphical form for the transmittance of the atmosphere over slant paths of various kinds. Salient features of the graphs and conclusions drawn from them are discussed.

The third chapter reports work in the second problem area, which is concerned with the operation of an optical communication channel under conditions of very low signal level at the receiver. The development of a statistical detection theory of square pulses, which began in Interim Report No. 4, continues with presentation of some numerical computations of the relevant statistical variables under various conditions of operation. The conclusion is drawn, that a larger reduction of the error probability results from a reduction of the bandwidth than from a corresponding lengthening of the pulse at constant bandwidth; for comparison, these two alternatives are equivalent in a classical channel. Another topic in this chapter is an error-reducing code; a "permutation code" is found to have some attractive features, but it does not appear to be adequate when the pre-decoding error rate is high.

The analysis of the properties of a laser amplifier as the first component after the lens system at the receiving end of a communication channel continues in this report, with emphasis on the selective properties of the amplifier.

The purpose of this analysis is to indicate whether or not such an amplifier can serve as an effective filter discriminating against a broad background radiation without adversely affecting the signals within the frequency band of the channel.

II. FIRST PROBLEM AREA ATMOSPHERIC ATTENUATION

2.1 Introduction

Transmittance tables for slant paths from altitudes of 15, 25, 30, and 50 km have been prepared by Plass (1963). The effects of absorption by CO_2 in the wave number range 500 to 10,000 cm^{-1} and water vapor (for wet and dry stratosphere models) between 1,000 and 10,000 cm^{-1} are considered. In this chapter we furnish some graphs based on these tables, so that implications may be more readily comprehended than from the tabulations.

2.2 Effect of CO_2

In this section certain conclusions from the information contained in Figs. 4 through 13 will be summarized. First of all, the conditions of relatively low transmittance occur in isolated spectral regions, such as 550-750 cm^{-1}, 2200-2500 cm^{-1}, 3400-3800 cm^{-1}, 1450-1750 cm^{-1}. At the centers of these regions, essentially complete opacity may be encountered for near-horizontal operation from an initial altitude of 15 km. One would conclude from those figures such as 8, 9, 10, 11 and 12, on which curves of a given spectral region for the same elevation angle but different transmitter altitudes are displayed, that there is improvement in transmittance, but still some loss, even for altitudes like 25 and 30 km, which might present practical difficulties as site locations. Transmittance values typically fall below 50 percent near the band centers. Although near-vertical transmittance is more dependable than low-angle (see Fig. 7 for an indication), this is a fact of little significance unless the trajectory of the object with which communication is desired can be controlled.

One might conjecture that use of finite bandwidth could improve transmittance by averaging over narrow lines. It is possible in principle to construct from Plass' tabulation a set of averages over any desired bandwidth, but such a task should be deferred until consideration of other factors, such as channel capacity, noise, equipment has indicated bandwidths for which computations are needed.

Meanwhile, we have presented in Fig. 4 an example of averaging,

taken from a table of Plass, in which the bandwidth is 50 cm^{-1}, or 1500 KMc. It appears that the transmittance is not improved at the band center, but the region of poor transmittance is widened, and is less sharply bounded than for the non-averaged curves. These conclusions are to be expected from the nature of averaging with bandwidth comparable to the width of the absorption region. Much larger bandwidths, if permitted by other considerations, might eliminate the problem of regions of poor transmittance. Bandwidths smaller than the 1500 KMc of the example are expected to have even less influence on the transmittance curves.

2.3 Water Vapor

The general character of the curves, as displayed in Figs. 1-3, is the same as for CO_2. High altitude sites and near-vertical inclination improve transmittance. We have chosen to base curves on the calculations made by Plass for the "dry atmosphere" model of Gutnick, since in any case the attenuation should not be less than predicted by this model. Regions of poor transmittance appear to exist for wave numbers 3570 - 3670 cm^{-1}, 3700 - 3900 cm^{-1}, and 5300 - 5400 cm^{-1}.

2.4 General Consideration on Absorption: Windows

We have seen that absorption within bands may be severe. In view of this fact and the difficulty of computing absorption profiles, it is imperative to circumvent the difficulty by deciding to operate in 'windows' between the regions of severe absorption. Such a decision is practical only if sufficient bandwidth is available in the windows. But since the relation between frequency and wavelength is

$$\lambda = c/\nu \ , \tag{2.1}$$

one has for the relation between two descriptions of bandwidth

$$\Delta\lambda = c/\nu^2 \Delta\nu = \frac{\lambda^2}{c}\Delta\nu \ , \tag{2.2}$$

MISSING PAGE

MISSING PAGE

MISSING PAGE

MISSING PAGE

MISSING PAGE

MISSING PAGE

MISSING PAGE

MISSING PAGE

MISSING
PAGE

MISSING PAGE

MISSING PAGE

MISSING PAGE

MISSING PAGE

so that, e.g., for a 1 KMc bandwidth at wavelength of N microns, the wavelength interval required is given by

$$\Delta\lambda = (N^2/3)10^{-5}\ \mu . \qquad (2.3)$$

Thus, there is adequate bandwidth available in the windows, which are usually determined from the solar spectrum to be (in microns) 0.95 - 1.05, 1.2 - 1.3, 1.5 - 1.8, 3 - 5. Some authors (Gaertner, 1957) list 8 - 10 as a window, but others (Howard and Garing, 1962) consider the O_3 band at 9.6μ to be a serious obstacle to transmission through the atmosphere, and the astronomer Goldberg (1954) refers to it as 'strong' so that 8 - 10μ should be rejected as a window until further study. It is clear that the windows listed allow bandwidths in excess of 1 KMc from application of criterion (2.3).

2.5 Rayleigh and Aerosol Attenuation

These two effects have been combined by Elterman (1963) into an 'optical thickness for the turbid atmosphere,' $\tau_t^{\infty}(h)$. In terms of this quantity, the slant path transmittance at zenith angle θ from altitude h to the edge of the atmosphere, as reduced by Rayleigh scattering and clear atmosphere aerosol attenuation, is given by

$$T_{h-\infty} = \exp - \left[\tau_t^{\infty}(h) \sec\theta \right] . \qquad (2.4)$$

Elterman tabulates this quantity $\tau_t^{\infty}(h)$ for wavelengths between 0.4μ and 4μ; it should not exceed the values computed for 4μ if larger wavelengths are employed. Since the transmittance from ground to aerospace at angles only 5^{o} above horizontal and 4μ wavelength may be calculated to exceed 90 percent from Elterman's tabulated value of $\tau_t^{\infty}(0) = 0.0489$ at 4μ, there appears to be no reason to consider the mechanism for attenuation further for $\lambda > 4\mu$. For smaller wavelengths, it can be significant at near-horizontal angles for transmission from ground or low altitudes, and the tabulations are accordingly reproduced here for λ between 0.4μ and 1.67μ.

TABLE I: TURBID OPTICAL THICKNESS

h(km)	τ_t^{∞}(h) 0.4μ	τ_t^{∞}(h) 0.5μ	τ_t^{∞}(h) 0.6μ	τ_t^{∞}(h) 0.7μ	τ_t^{∞}(h) 0.9μ	τ_t^{∞}(h) 1.67μ
0	0.4977	0.2661	0.1813	0.1394	0.1057	0.0771
1	0.3707	0.1771	0.1079	0.0761	0.0514	0.0338
2	0.2973	0.1312	0.0727	0.0468	0.0273	0.0151
3	0.2494	0.1051	0.0546	0.0328	0.0165	0.0071
4	0.2134	0.0877	0.0438	0.0250	0.0112	0.0035
5	0.1843	0.0747	0.0364	0.0202	0.0083	0.0019
6	0.1600	0.0645	0.0312	0.0171	0.0068	0.0013
7	0.1389	0.0559	0.0270	0.0148	0.0058	0.0010
8	0.0893	0.0484	0.0234	0.0128	0.005	0.0009
9	0.0765	0.0418	0.0202	0.0111	0.0044	0.0008

III. SECOND PROBLEM AREA: INFORMATION EFFICIENCY AND CHOICE OF DETECTION SYSTEM

3.1. Introduction

The second problem area concerns the possibility and the means for operating an optical communication channel with an average signal power at the receiving end of less than one energy quantum per sample of the modulated light wave. The crucial points are the choice of systems of coding and modulation at the transmitter and of detection and decoding at the receiver. First priority has been given to the investigation of channels operating with a photon-counting detector.

The technical and economical drawbacks connected with attempting reliable communication at such low signal levels has been emphasized in previous reports. The basic uncertainty and error probability of such a channel requires very complicated codes and expensive terminal equipment for coding and decoding, which are yet to be developed.

In the Interim Report No. 4 (Hok et al, 1965) the analysis of an approach to an effective code for such a channel was begun by breaking the error-reduction problem up into two steps. The first step was to lump a number of the samples into pulse digits; the error probability for the detection of such a digit by a photon counter was shown to be obtainable by statistical decision theory. The result showed some interesting similarities and dissimilarities with the classical channel perturbed by white Gaussian noise.

In the present report this line of investigation is continued. Some numerical calculations on an electric computer add some quantitative results. It is shown that a reduction of the bandwidth of the channel is a more effective way of reducing the error rate than an increase in the pulse length at constant bandwidth.

The choice of bandwidth is thus a basic compromise between channel capacity and pre-decoding error probability. In this report an attempt is made to find a rough upper bound for the channel bandwidth beyond which the channel capacity increases too slowly for any reasonable application. At this extremum

of the bandwidth and a background temperature of $300^{o}K$, the marginal signal level would be 10^{-22} and 0.3 photons per sample, respectively, at the wavelength limits 0.4 and 20 microns.

The second step in the process of solving the coding problem is also considered in this chapter, i.e. the design of an error-correcting code for a highly asymmetric binary channel. The coding-decoding procedure presented here is a variation of the recently published permutation principle (Slepian, 1965). However, it does not seem to offer any simple solution to the error reduction of signals with the extremely high error rates at operation in the range of a fraction of a photon per sample.

In the last section of this chapter we are continuing the study of a laser amplifier as a component of an optical communication channel. The previous calculations emphasized the amplifier gain and the fluctuations added to the amplified signal. However, the approximations made excluded the consideration of the variation of the gain of the amplifier over the signal bandwidth. In the present report damping-theory techniques are used to obtain a finite amplitude bandwidth and a continuous relation between gain and frequency, so that the discrimination of the amplifier against broad background radiation can be estimated.

3.2 Channel Capacity and Bandwidth

It is intuitively obvious that the channel capacity for given average signal power and white noise power density must be a monotone nondecreasing function of the available bandwidth. Increasing the frequency band available for channel use cannot very well reduce the maximum rate of transmission of information. Nonetheless it is possible to discuss an "optimum" bandwidth, since the signal-to-noise ratio decreases with increasing bandwidth; the processing of a larger number of data per second, where each point has a broader error distribution, requires a more complicated code and costlier terminal equipment.

The classical channel capacity in the presence of white Gaussian noise

$$C = \Delta f \log (1 + \frac{S}{N_o \Delta f}) \tag{3.1}$$

may be rewritten

$$C \cdot \frac{N_o}{S} = \frac{\Delta f}{\Delta f_m} \log (1 + \frac{\Delta f_m}{\Delta f}) \tag{3.2}$$

which approaches unity asymptotically with increasing bandwidth. The righthand side of (3.2) has one single parameter Δf_m which is the bandwidth for which the signal-to-noise ratio is unity. At this bandwidth this dimensionless capacity is $\log 2 = 0.69$ of the asymptotic value one.

The partially quantum-limited channel has a capacity with an additional parameter $\mu = N_o/\hbar\omega$.

$$C = \Delta f \left\{ \log (1 + \frac{S}{N_o + \hbar\omega) \Delta f}) + \frac{S + N_o \Delta f}{\hbar\omega \Delta f} + \log (1 + \frac{\hbar\omega}{S + N_o \Delta f}) - \frac{N_o}{\hbar\omega} \log (1 + \frac{\hbar\omega}{N_o}) \right\} \tag{3.3}$$

Introducing a corresponding dimensionless variable

$$\sigma = \frac{\Delta f_g}{\Delta f} = \frac{S}{\hbar\omega \cdot \Delta f}$$

we obtain

$$C \cdot \frac{\hbar\omega}{S} = \frac{1}{\sigma}\left\{\log\left(1+\frac{\sigma}{1+\mu}\right) + (\mu+\sigma)\log\left(1+\frac{1}{\mu+\sigma}\right) - \mu\log\left(1+\frac{1}{\mu}\right)\right\}. \qquad (3.4)$$

This dimensionless channel capacity increases monotonically from 0 at $\Delta f = 0\,(\sigma = \infty)$ to $\log\left(1+\frac{1}{\mu}\right)$ for $\Delta f = \infty\,(\sigma = 0)$.

By algebraic manipulations (3.4) may be transformed to

$$C \cdot \frac{\hbar\omega}{S} = \log\left(1+\frac{1}{\mu+\sigma}\right) + \frac{1}{\sigma}\log\frac{\left(1+\frac{1}{\mu+\sigma}\right)^{1+\mu}\left(1+\frac{\sigma}{\mu}\right)}{\left(1+\frac{1}{\mu}\right)^{1+\mu}}. \qquad (3.5)$$

Here the first term has the asymptotic values quoted above, while the second term is zero at both limits. The first term reaches a value of half the asymptotic limit

$$\log\left(1+\frac{1}{\mu+\sigma_h}\right) = \frac{1}{2}\log\left(1+\frac{1}{\mu}\right) \qquad (3.6)$$

for the bandwidth

$$\Delta f_h = \frac{S}{\sigma_h \hbar\omega} = \left[\mu(1+\mu)\right]^{-1/2} \cdot \frac{S}{\hbar\omega} = \frac{S}{\sqrt{N_o(\hbar\omega+N_o)}} \qquad (3.7)$$

At this point the second term is not negligible; for $\mu \lesssim 1$ it is positive and reaches values up to about half the value of the first term. However, since the first term is by far dominant and the sum is monotone, the bandwidth (3.7) may be taken as a rough indication of the point beyond which the payoff in channel capacity will necessarily become small compared to the cost of coding complexity. Since the measure is rough and of interest primarily in the strongly quantum-limited frequency range where μ is small, it may be more appropriate to write:

$$\Delta f_h = \frac{S}{\sigma_h \hbar\omega} \approx \mu^{-1/2} \cdot \frac{S}{\hbar\omega} = \frac{S}{\sqrt{\hbar\omega N_o}}. \qquad (3.8)$$

Since no known practical codes approach the channel capacity with negligible error probability, it is necessary to settle for a rate of transmission of information considerably below the ideal capacity. The discussion above suggests that given a wide band channel the first unsophisticated coding operation that may be performed is to reduce the bandwidth of the signal. Close to the asymptotic capacity a substantial increase in signal-to-noise ratio and reduction in error probability can be obtained with only a moderate loss in theoretical capacity.

If (3.7) is accepted as the upper limit of useful bandwidth, the number of signal photons per sample in a marginal channel

$$n_s = \mu(1+\mu). \tag{3.9}$$

At the crossover point between noise-limited and quantum-limited channels ($\mu = 1$), which for a temperature of 290°K occurs in the infrared at a wavelength of $72\,\mu$, $n_s = 1.4$. In the wavelength range of this project 0.4 to $20\,\mu$, the marginal number of photons per sample varies from 10^{-22} to 0.3. The theoretical channel capacity under these conditions varies approximately from 45.5 $S/\hbar\omega$ to 1.1 $S/\hbar\omega$ bits, respectively, i.e. roughly fifty to one bit, respectively, multiplied by the average number of received signal photons per second.

It is doubtful that it will be practically and economically justifiable to design optical communication links for as large bandwidths and as small photon numbers per sample as indicated by the marginal conditions discussed above.

3.3 Signal Detection and Error Statistics

In order to realize as nearly as possible without errors a rate of transmission equal to the theoretical channel capacity, the following design problems have to be solved:

1. The choice of methods of modulation and detection, as well as the optimization of the components implementing them.

2. The design of an error-detecting code suitable for the channel, as well as corresponding encoder and decoder.

The analysis of the first-mentioned problem in the Interim Report No. 4 proceeded from the assumption that a binary modulation would be used, one digit consisting of a specified combination of samples, the other digit being a space, no signal at all. For each unit time interval equal to the duration of one digit, the receiver then has to perform a binary decision, one or zero, signal or no signal. The result is a quantum-mechanical modification of the classical theory of detection of a known signal in white Gaussian noise. While the classical theory finds the logarithm of the likelihood ratio to be a monotone function of the (linear) correlation between the receiver input and the known signal, the quantum theory gives this logarithm as a monotone function of a certain "nonlinear correlation" between the output of a "photon counter" and the envelope of the known signal. This nonlinear correlation index is the second summation in the expression for the logarithm of the likelihood ratio (Eq. 3.21 in Interim Report No. 4).

$$\log\left[\ell(r)\right] = -\mu\sum_i \gamma_i + \sum_i \log \mathcal{L}_{r_i}(-\gamma_i) = -A + \alpha \qquad (3.10)$$

where the number i runs over all the envelope samples, $\mathcal{L}_r(x)$ is the Laguerre polynomial of x of order r and

$$\gamma_i = \frac{S_i^2}{2N(1+\mu)} \,. \qquad (3.11)$$

Here S_i is the i^{th} sample of the known signal envelope, $N = N_o \Delta f$ is the power of the thermal background radiation within the frequency band Δf occupied by the signal, and finally

$$\mu = \frac{N_o}{\hbar\omega} \qquad (3.12)$$

is the ratio of the spectral density of the background radiation to the photon energy.

For simplicity we assumed in the previous report that the signal was a square pulse, so that all the samples $\gamma_i = \gamma$. If n_k is the number of samples in the pulse, then

$$A = \mu n_k \cdot \gamma = \frac{L(S)\mu}{N_o(1+\mu} \tag{3.13}$$

$$\alpha = \sum_{i=1}^{n_k} \log \mathcal{L}_{r_i}(-\gamma) \tag{3.14}$$

and all the random variables r_i have the same statistics; also all the terms in the summation (3.14) are random variables with identical distributions. If n_k is reasonably large, the distributions of α in the presence and in the absence of a signal are approximately Gaussian with the same variance but different means. It was shown in the previous interim report that the means m_1 in the absence of a signal and m_2 in the presence of a signal are related to the variance σ^2 and the quantity A in (3.13) by the equations

$$m_1 = A - \frac{1}{2}\sigma^2$$

$$m_2 = A + \frac{1}{2}\sigma^2 \quad . \tag{3.16}$$

Since A is easily evaluated, one of the quantities m_1, m_2, σ^2 must be determined in order to specify the approximate distribution functions of α. We have obtained numerical values of $\frac{m_1}{n_k}$, by means of a digital computer

$$\frac{m_1}{n_k} = \frac{1}{n_k} E_{S_o}(\alpha) = \sum_{r=0}^{\infty} \frac{\mu^r}{(1+\mu)^{r+1}} \log \mathcal{L}_r(-\gamma) \quad . \tag{3.17}$$

The result is plotted vs γ for various values of μ in Fig. 14..

Except for the choice of a threshold value α_c for the decision signal-no signal the error probabilities depend on only one parameter σ, provided that n_k is large enough for the Gaussian approximation to be satisfactory. Fig. 15. shows qualitatively the relationship between the two distribution functions in terms of the normalized argument α/σ. The curves are displaced a distance σ from each other. The single parameter σ is easily found from (3.15).

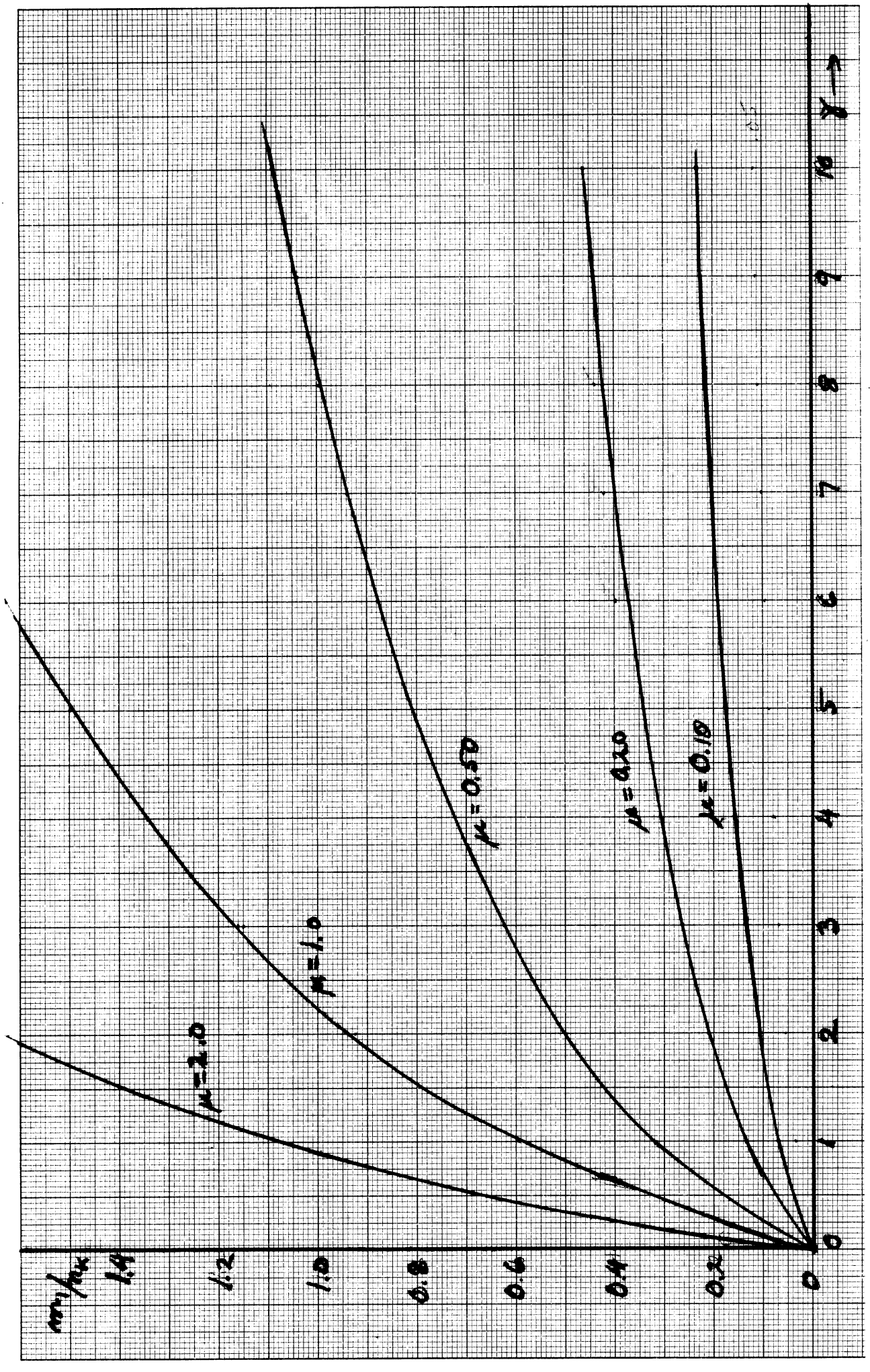

FIG. 14: Mean Value of α/n_k (no signal).

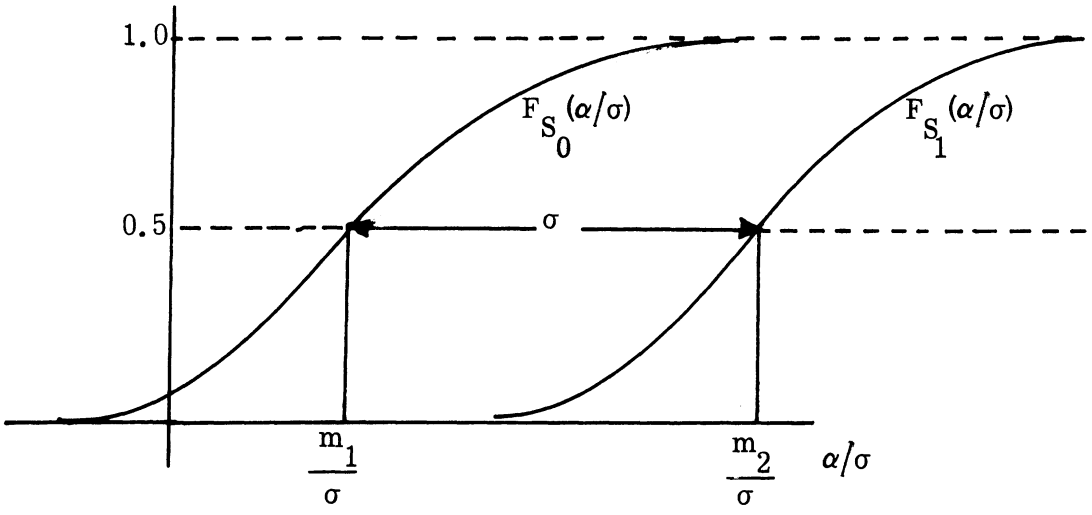

FIG. 15:: Distribution Functions of α/σ .

$$\sigma = \sqrt{2A\left(1 - \frac{m_1}{A}\right)} = \sqrt{2n_k \gamma_\mu \left(1 - \frac{m_1}{n_k \gamma \mu}\right)} \quad . \tag{3.18}$$

The first factor

$$\sqrt{2A} = \left[\frac{2L(S)}{N_o + \hbar\omega}\right]^{1/2} \tag{3.19}$$

corresponds very closely to the single parameter $2L/N_o$ in the classical detection problem, the only difference being the $\hbar\omega$ added in the denominator. The important qualitative difference between the classical and the quantum-controlled detection problem is expressed by the second factor

$$\sqrt{1 - \frac{m_1}{A}} = \sqrt{1 - \frac{m_1}{n_k \gamma \mu}} \tag{3.20}$$

which severely reduces the distance between the two distributions for small values of γ. Fig. 16 gives the square of this factor for $\mu = .05$ and 1.0, respectively, plotted vs γ. In Fig. 17 $\sigma^2/2n_k$ is shown as a function of γ for a few values of μ.

It is seen from Fig. 16 that the factor (3.20) is not very strongly affected by the value of μ except at very small values of γ.

When the Gaussian approximation is good enough, the above results make it now possible to calculate, at least numerically, the error probabilities for any chosen threshold value $\ell(r) = \lambda_c$. The receiver operating characteristic (Fig. 3-2 in Interim Report No. 4) is a convenient graph for presenting this information in compact form. The coordinates in this diagram are the conditional complementary distribution functions

$$x = P_{S_o}(\ell(r) \geq \lambda_c) = P_{S_o}(F) = 1 - F_{S_o}(\lambda_c) = \int_{\alpha_c}^{\infty} \frac{1}{\sqrt{2\pi\sigma^2}} \exp\left(-\frac{(\alpha - m_1)^2}{2\sigma^2}\right) d\alpha \tag{3.21}$$

$$y = P_{S_1}(\ell(r) \geq \lambda_c) = P_{S_1}(H) = 1 - F_{S_1}(\lambda_c) = \int_{\alpha_c}^{\infty} \frac{1}{\sqrt{2\pi\sigma^2}} \exp\left(-\frac{(\alpha - m_2)^2}{2\sigma^2}\right) d\alpha \quad . \tag{3.22}$$

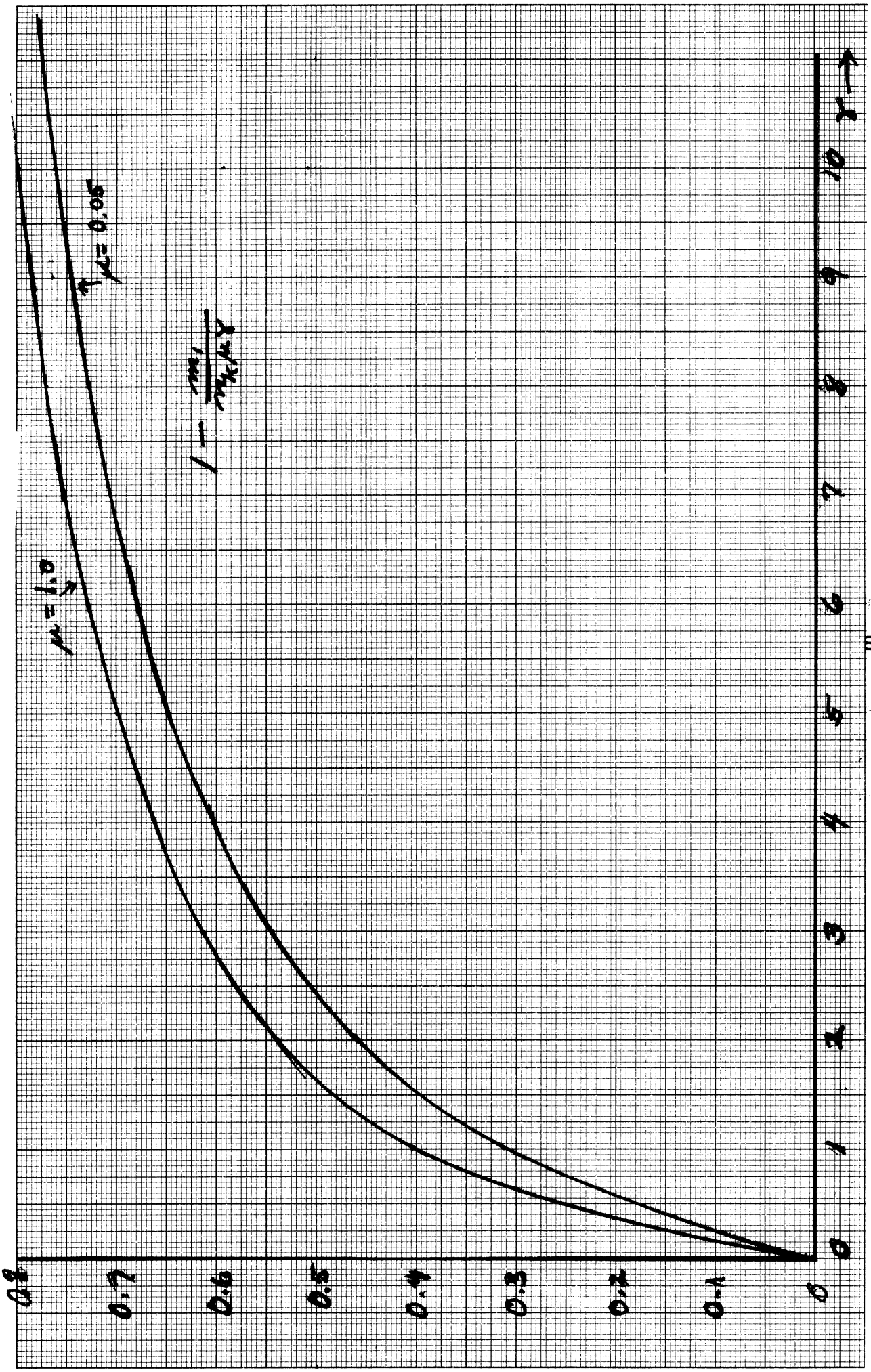

FIG. 16: Graph of the factor $\left[1 - \frac{m_1}{n_k \mu \gamma}\right]$.

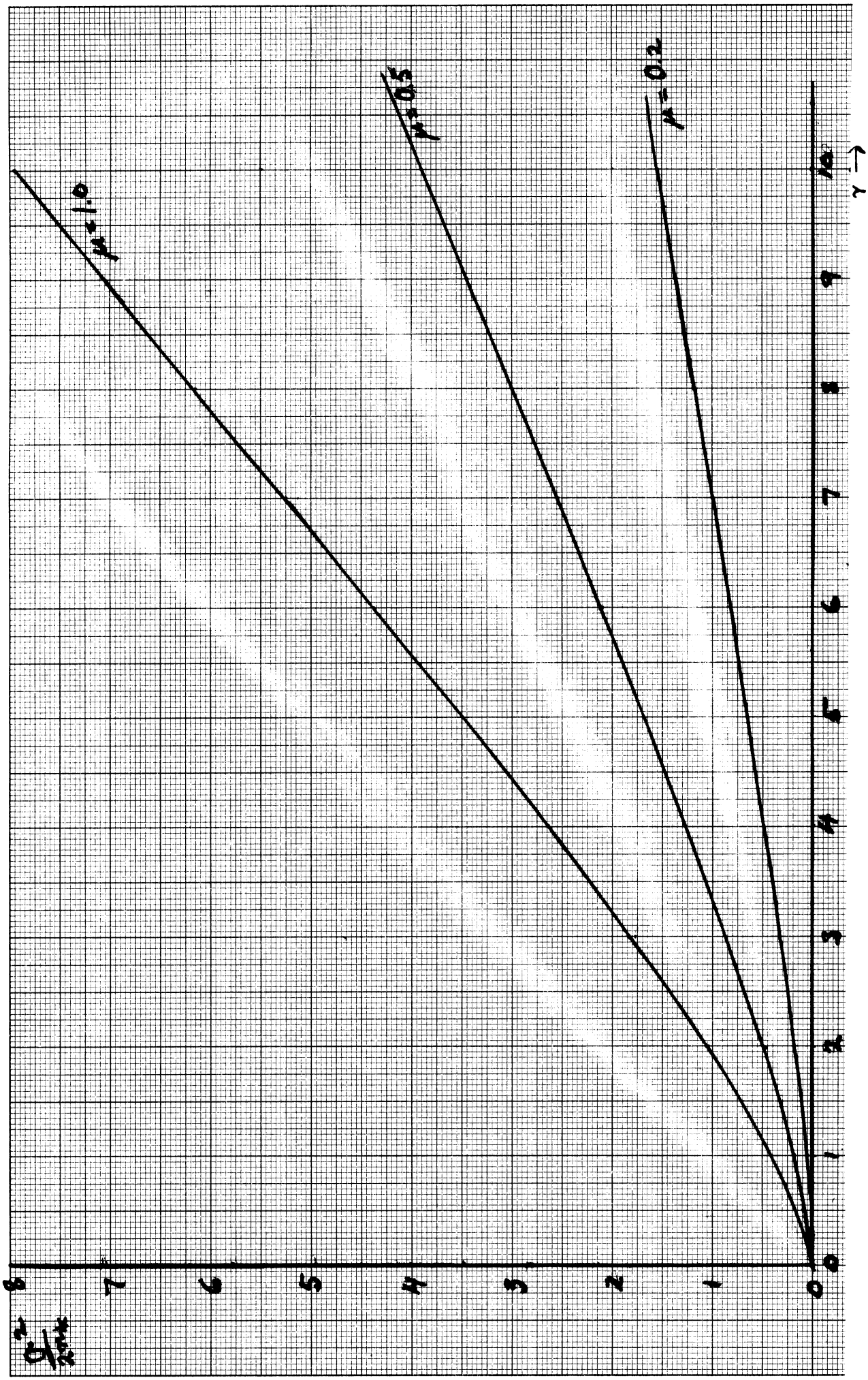

FIG. 17: The Variance of the Logarithm of the Likelihood Ratio.

Because of the relations between m_1, m_2 and σ, this diagram has one single parameter σ, which determines the error statistics for any chosen value of λ_c.

The optimization of the channel for given prior probabilities of a pulse of given length or no pulse may use a minimum total error rate, i.e. false alarms plus misses, as the criterion; a more satisfactory criterion for a communication channel is the minimum equivocation

$$H_e = -P(1)\left\{ p(H)\log p(H) + \left[1 - p(H)\right]\log\left[1 - p(H)\right]\right\} - P(0)\left\{ p(F)\log p(F) + \left[1 - p(F)\right]\log\left[1 - p(F)\right]\right\} \tag{3.23}$$

obtained by varing the threshold value λ_c of the likelihood ratio.

Setting the derivative $\frac{dH_e}{d\alpha_c} = 0$ leads to the following relation in terms of the coordinates of the receiver operating characteristic:

$$\log\frac{1-x}{x}\,\frac{\log\frac{y}{1-y}}{\log\frac{1-x}{x}}\cdot\frac{dy}{dx} = \frac{1-P(1)}{P(1)} \tag{3.24}$$

Numerically-graphically this equation may be solved by taking data point by point from the graph, computing the left number and plotting it versus x. The stationary points of the equivocation are found as the intersections of the plotted curve with the horizontal line representing the right number of (3.24). The intersection for which

$$0 < x < 0.5 \tag{3.25}$$

$$0.5 < y < 1 \tag{3.26}$$

indicates the x-coordinate for which the minimum equivocation occurs. In this interval the left member of (3.24) has no singularities and is monotone increasing.

The primary purpose of the present analysis of the statistics of detection of coherent optical signals with a thermal background radiation was to investigate the reduction of error probability by introducing the simplest possible redundancy,

i.e. by lengthening the signal digit pulse. The result was given by (3.18), indicating that the parameter σ, which is a positive performance indicator, increases with the square root of the number of samples in the pulse, just as in the classical detection theory. However, σ depends not only on the ratio of the pulse energy to the total noise spectral density, as in the classical case. The factor presented in (3.20), which has no classical analog, introduces a dependence on γ illustrated by Fig. 16. Since γ is inversely proportional to the bandwidth, it is more advantageous to reduce the bandwidth than to increase the pulse length at constant bandwidth if γ is small.

For such wide-band low-power communication channels which require an extremely small probability of error without appreciable loss of rate of transmission of information, it is consequently necessary to start with a bandwidth of the order of (3.7) and to apply a highly sophisticated coding and decoding system on the basis of single-sample pulses.

When a moderate loss of rate of transmission can be tolerated, it is more economical to start from a considerably smaller bandwidth, so that the pre-coding error rate is reasonable and a rather simple code can be used for further error reduction.

3.4 Error-Reducing Codes

The problem of devising an error-reducing code for a binary channel with the general properties discussed in preceding sections is based on the following postulates:

1) A binary channel with a fixed bandwidth, pulse length and noise background is given,
2) Both peak and average signal power is assumed known, so that the duty factor or prior pulse probability P(1) is fixed.
3) A likelihood-ratio receiver is used.

On the basis of these postulates the two distribution functions for the logarithm of the likelihood ratio, i.e. the receiver operating characteristic,

is completely specified.

If the prior pulse probability is not determined by the characteristics of the laser transmitter, it may be optimized by variational methods. For single-sample pulses this subject has been treated by Gordon (1962) and reviewed in our first interim report (Barasch et al, 1964).

It has been pointed out several times in the previous reports that since in general $P(1) << 1/2$ the binary channel is highly asymmetric and that so far very little work has been devoted to codes for such channels. However, since the writing of the March interim report a new coding-decoding principle has been presented in the literature (Slepian, 1965), which lends itself very well to the coding of asymmetric binary channels. We shall here briefly discuss the general principle involved in its binary form[1] and consider its application to optical channels, as well as an extension of the principle for the purpose of reducing further the error probability.

Slepian has named the principle "permutation modulation," since it may be considered a generalization which includes as special cases some of the known forms of pulse modulation codes.

When the "on" probability P(1) is given, any "word" or block of N independent digits will contain on the average $M = N \cdot P(1)$ pulses. A code built on the permutation-modulation principle uses words all of the same length N and with exactly M pulses. The ensemble of words in the code is thus all possible permutations of M pulses and N - M spaces. For large N the restriction of using only these words is not a very severe one. The relation that the number of pulses in each group is equal to M is analogous to the parity equation in a simple parity code but it gives a more specific constraint on the digits of the word.

The first step in the decoding process is to assign pulses to the M unit intervals in each word which show the largest likelihood ratios. This gives the

---

[1] The code described here differs somewhat from the two variants Slepian discusses because we are here concerned with envelope samples or pulse envelopes, which are always positive, while Slepian's classical channel has both positive and negative samples.

maximum-likelihood estimate of the transmitted word that produced each received word. These estimates are all members of the word ensemble and can be decoded on a one-to-one basis.

Because of the homogeneous structure of the code, the error probability is the same for all words. The error probability may be evaluated in terms of a multi-dimensional space with one dimension corresponding to each digit in a word. A received signal produced by a transmitted code word can be associated with a point in this space. The coordinates may conveniently be the values of the variable

$$\eta = \frac{\alpha - A}{\sigma} \tag{3.27}$$

for each digit in the word. The variance of this variable is always unity; its mean is zero if the digit is zero and σ if the digit is one. There is a one-to-one correspondence between the code words and those uniformly distributed points on a sphere, which have N - M coordinates equal to zero and M coordinates equal to σ. The one of these points located within the shortest distance of the received-signal point identifies the maximum likelihood estimate of the transmitted word, which would be found by the decoding procedure described earlier in this section. Integrating the probability density of the received point over the volume in N-space, where no other word point is closer, we obtain the probability that the estimate is correct, i.e. one minus the error probability. Since the α-distribution has been assumed known, this probability can be calculated in this way. In the case of an acceptable Gaussian approximation (multisample pulses), the calculation procedure is exactly the same as in Slepian's classical channel, which will not be discussed here at the present time.

It has been pointed out previously that the "constraint equation" is somewhat analagous to the parity equation of a simple parity-check code. This analogy suggests immediately that the permutation code can be equipped to correct a larger number of errors by imposing additional constraints of the same nature, according to the same general patterns developed for parity codes. As an example, let us

form a rectangular matrix from N_w subsequent permutation code words stacked vertically

$$\begin{vmatrix} D_{11} & D_{12} \cdots\cdots & D_{1N_d} \\ D_{21} \cdots\cdots & & \\ \vdots & & \\ D_{N_w 1} \cdots\cdots & & D_{N_w N_d} \end{vmatrix} \tag{3.28}$$

and restrict the word sequences as well as the digits within each word by the constraint equations

$$\sum_{j=1}^{N} D_{ij} = M_d \tag{3.29}$$

$$\sum_{i=1}^{N} D_{ij} = M_w \tag{3.30}$$

where

$$\frac{N_d}{M_d} = \frac{N_w}{M_w} \tag{3.31}$$

Effectively the word length of this code is $N_d \cdot N_w$ rather than N_d, and the rate of transmission of information per digit has been considerably reduced by the added constraints.

The first decoding step as described above now produces two digit matrices, one by assigning M_d pulses to the digits with highest likelihood ratio in each row and one by assigning in the same way M_w pulses to each column. Differences between the two matrices indicate errors. The most likely error is a reversal of the order

between the M^{th} and the $(M+1)^{th}$ digit in a row or column, when the digits are numbered in order to decreasing likelihood ratio. If the two matrices can be brought to coincidence by interchange of such borderline digits, the result is intuitively the maximum-likelihood estimate. If more than one result can be obtained by this operation, the one involving the smallest differences in likelihood-ratio at the interchanges is the preferred estimate.

This rather simple class of codes does not appear to be able to cope with channels where the signal-to-noise ratio is low and the pre-decoding error rate high, even if redundancy is increased by choosing rather small N_s and by going to three-dimensional and higher matrices. Much more sophisticated codes will have to be developed before reliable communication can be obtained under such circumstances.

3.5 Gain Selectivity of Quantum Amplifiers

3.5.1 Introduction

In a previous Interim Report (Hok et al, April 1965), we developed the theory of a quantum amplifier and studied the amplification of the energy as well as the field amplitudes of a single mode of the radiation field. The active material was assumed to have two sharply defined energy levels. Because of this assumption, the gain, as a function of frequency, contains a δ-function. This implies that if the frequency of the signal does not coincide with the frequency of transition between the two levels, the signal will not be affected by the amplifier. Of course, this is true if all other processes by which the signal can be affected are neglected. This idealization is not bad if we confine the signal inside a relatively narrow bandwidth about an optical or infrared frequency. And it is a better approximation for a gaseous material than it is for a solid state material.

The assumption of sharply defined energy levels is an idealization in itself since the active material will always be in interaction with, if nothing else, the vacuum radiation field. Such interactions give rise to broadening of the energy levels of the active material. Thus, one expects the gain to be a more or less

peaked function of frequency. If this is so, the laser preamplifier can presumably be used as a filter to improve the signal to noise ratio whenever external noise is present. This is the objective of the present study.

To account for broadening in a quantum mechanically consistent manner is a rather intricate problem, and requires considerable formal development. We have used the techniques of damping theory which has been proven to be very useful in the study of line broadening phenomena (see e.g. Akcasu, 1963). The details of the formal mathematical development are not presented here since they will appear in the final report. We present only the basic steps and devote most of the discussion to the analysis of the filtering properties of the laser preamplifier. Finally, we present the solution of the equations for the matrix elements of the density operator of the field mode.

3.5.2 Time Evolution of the Density Operator

As discussed in Interim Report 06515-4T, let H^A be the Hamiltonian of the active material, $H^R = \hbar\omega(a^\dagger a + 1/2)$ the Hamiltonian of the field mode, and $V^r = d(a^\dagger + a)$, the interaction between the two. Let, in addition, H^P be the Hamiltonian of a third system, which shall be referred to as "the perturber" and V^c the interaction between (A) and (P). It is assumed that the perturber interacts with the active material only and not with the field mode. This interaction V^c causes the broadening of the levels of H^A. Later, we will indicate how the interaction with the vacuum radiation field can be included in V^c.

Now, we define

$$H^B \equiv H^A + H^P + V^c \tag{3.32}$$

and

$$H^o \equiv H^B + H^R \quad . \tag{3.33}$$

Then, the total Hamiltonian reads

$$H = H^o + V^r \quad . \tag{3.34}$$

The time evolution operator of the whole system is:

$$U(t) = e^{-\frac{i}{\hbar}Ht} , \tag{3.35}$$

and the time evolution of the total density operator is governed by

$$\rho(t+\tau) = U(\tau)\,\rho(t)\,U^{\dagger}(\tau) . \tag{3.36}$$

Let $|n\rangle$ be the eigenstates of H^R defined by

$$a^{\dagger}a\,|n\rangle = n\,|n\rangle , \qquad n = 0, 1, 2 \ldots \tag{3.37}$$

and $|\beta\rangle$ the eigenstates of H^B, i.e.

$$H^B\,|\beta\rangle = E_\beta\,|\beta\rangle . \tag{3.38}$$

To determine these eigenstates is a difficult problem in itself. What we know is that H^A is a two-level system with known eigenstates and that H^P has a continuous spectrum. It should be noted that H^P may consist of several parts. At least one of them must have a continuous spectrum. The eigenstates of H^P are also assumed to be known. Then, with V^c also known, one has to solve the eigenvalue problem (3.38). In this study we will not need to know the precise form of the eigenstates $|\beta\rangle$. It will suffice to make use of some of the properties that they are expected to have. This is possible because we are not interested in the details of the line shape at this stage. If, however, one wishes to find the precise form of the gain as a function of frequency for a specific active material, knowledge of H^P and V^c, as well as the solution of (3.38) will be necessary.

We now define the reduced density operator

$$\rho^R \equiv \mathrm{Tr}_B\,\rho = \sum_{\beta} \langle\beta|\,\rho\,|\beta\rangle . \tag{3.39}$$

Considering a specific matrix element of ρ^R, we have

$$\rho^R_{mn}(t+\tau) = \sum_{\beta} \langle m\beta|\,U(\tau)\,\rho(t)\,U^{\dagger}(\tau)\,|n\beta\rangle . \tag{3.40}$$

Taking $\rho(t) = \rho^R(t)\,\rho^B(t)$ and after some manipulation we obtain

$$\rho^R_{mn}(t+\tau) = \rho^R_{mn}(t) \sum_{\beta} \langle m\beta | U(\tau) | m\beta \rangle \rho^B_{\beta\beta} \langle n\beta | U^{\dagger}(\tau) | n\beta \rangle$$

$$+ \sum'_{m_1 m_2} \rho^R_{m_1 m_2} \sum'_{\beta\beta_1} \langle m\beta | U(\tau) | m_1\beta_1 \rangle \rho^B_{\beta_1\beta_1} \langle m_2\beta_1 | U^{\dagger}(\tau) | n\beta \rangle . \qquad (3.41)$$

The Dirac ket and the subscript notations for matrix elements will be used interchangeably and at convenience throughout this report. Note that terms containing diagonal matrix elements of U combined with off-diagonal matrix elements of $U^{\dagger}$, and vice versa, do not appear in Eq. (3.41) since they vanish as we have seen in the previous Interim Report. To simplify the discussion, let us introduce

$$A^{mn}(\tau) \equiv \sum_{\beta} \langle m\beta | U(\tau) | m\beta \rangle \rho^B_{\beta\beta} \langle n\beta | U^{\dagger}(\tau) | n\beta \rangle \qquad (3.42)$$

and

$$C^{mn}_{m_1 m_2}(\tau) \equiv \sum'_{\beta\beta_1} \langle m\beta | U(\tau) | m_1\beta_1 \rangle \rho^B_{\beta_1\beta_1} \langle m_2\beta_1 | U^{\dagger}(\tau) | n\beta \rangle . \qquad (3.43)$$

The primes on the summation symbols indicate that equal values of the dummy indices are excluded. Thus, Eq. (3.41) becomes

$$\rho^R_{mn}(\tau) = \rho^R_{mn} A^{mn}(\tau) + \sum_{m_1 m_2} \rho^R_{m_1 m_2} C^{mn}_{m_1 m_2}(\tau) \qquad (3.44)$$

Now, the problem is to compute A and C. In the previous report, we used conventional perturbation theory to calculate the matrix elements of $U(\tau)$. Here, we shall proceed differently, for two reasons. First, the conventional perturbation theory has the unpleasant feature that it does not take into account the decay of the initial state and this may lead to inconsistencies. Second, we wish to account for broadening, and this cannot be done by means of perturbation theory. Actually, the two reasons are interrelated. Damping theory, as discussed in (Akcasu, 1963)

or (Messiah, 1964) gives us expressions for the diagonal and off-diagonal matrix elements of $U(\tau)$. These expressions are:

$$\langle m\beta \mid U(\tau) \mid m\beta \rangle = e^{-i(m\omega+\omega_\beta + S_{m\beta} - i\Gamma_{m\beta})\tau}, \tag{3.45}$$

and

$$\langle m\beta \mid U(\tau) \mid m'\beta' \rangle = \langle m\beta \mid V^r \mid m'\beta' \rangle \int_0^\tau dt \langle m\beta \mid U(\tau-t) \mid m\beta \rangle$$

$$\langle m'\beta' \mid U(t) \mid m'\beta' \rangle \tag{3.46}$$

where

$$S_{m\beta} = \hbar^{-1} \langle m\beta \mid V^r \mid m\beta \rangle + \mathcal{P} \sum_{m'\beta' \neq m\beta} \frac{\hbar^{-1} \left| V^r_{m'\beta', m\beta} \right|^2}{E_{m\beta} - E_{m'\beta'}}, \tag{3.47}$$

$$\Gamma_{m\beta} = \frac{\pi}{\hbar} \sum_{m'\beta' \neq m\beta} \left| V^r_{m'\beta', m\beta} \right|^2 \delta(E_{m\beta} - E_{m'\beta'}) \tag{3.48}$$

and

$$\omega_\beta = \frac{E_\beta}{\hbar}. \tag{3.49}$$

Due to the fact that $V^r = d(a^\dagger + a)$ and the known properties of $a^\dagger$ and a the matrix element $\langle m\beta \mid V^r \mid m\beta \rangle$ appearing in Eq. (3.47) vanishes. The symbol $\mathcal{P}$ in that same equation indicates the Cauchy principal value. The quantity d has been defined in the previous report. It represents the constant coupling the field mode to the active material. For convenience, we shall use the quantity D defined by $D = \hbar^{-1} d$. It will also be convenient to introduce the complex quantity

$$\gamma_{m\beta} = S_{m\beta} - i\Gamma_{m\beta}. \tag{3.50}$$

After a considerable amount of mathematical manipulation we obtain the following equation:

$$\rho^{R}_{mn}(t+\tau) = e^{-i(m-n)\omega\tau}\left[\rho^{R}_{mn}(t)\sum_{\beta}\rho^{B}_{\beta\beta}\, e^{-i(\gamma_{m\beta}-\gamma^{*}_{n\beta})\tau}\right.$$

$$+\sqrt{(m+1)(n+1)}\,\rho^{R}_{(m+1)(n+1)}(t)\sum_{\beta\beta_1}{}'\rho^{B}_{\beta_1\beta_1}\,|D_{\beta\beta_1}|^2\,J^{(+)}_{\beta\beta_1}(\tau)+$$

$$\left.+\sqrt{mn}\,\rho^{R}_{(m-1)(n-1)}(t)\sum_{\beta\beta_1}{}'\rho^{B}_{\beta\beta_1}\,|D_{\beta\beta_1}|^2\,J^{(-)}_{\beta\beta 1}(\tau)\right], \qquad (3.51)$$

where the quantities $J^{(\pm)}_{\beta\beta_1}$ are given by

$$J^{(\pm)}_{\beta\beta_1}(\tau) = e^{-i(\gamma_{m\beta}-\gamma^{*}_{n\beta})\tau}$$

$$\frac{\left[e^{-i\left(\pm\omega-\omega_{\beta}+\omega_{\beta_1}-\gamma_{m\beta}+\gamma_{(m\pm1)\beta_1}\right)\tau}-1\right]\left[e^{-i\left(\pm\omega-\omega_{\beta}+\omega_{\beta_1}-\gamma^{*}_{n\beta}+\gamma^{*}_{(n\pm1)\beta_1}\right)\tau}-1\right]}{\left(\pm\omega-\omega_{\beta}+\omega_{\beta_1}-\gamma_{m\beta}+\gamma_{(m\pm1)\beta_1}\right)\left(\pm\omega-\omega_{\beta}+\omega_{\beta_1}-\gamma^{*}_{n\beta}+\gamma^{*}_{(n\pm1)\beta_1}\right)}$$

To develop a differential equation for $\rho^{R}_{mn}(t)$, we expand the exponential of the first term of Eq. (3.51) and retain only the first two terms, i.e.

$$e^{-i(\gamma_{m\beta}-\gamma^{*}_{n\beta})\tau} \simeq 1-i(\gamma_{m\beta}-\gamma^{*}_{n\beta})\tau\ . \qquad (3.53)$$

This is justified by the fact that we assume the amplification to be linear. Recall that $\gamma_{m\beta}$ is proportional to $|D|^2$ which is the coupling constant. The same exponentials are involved in the expression for

$$J^{(\pm)}_{\beta\beta_1}(\tau)\ .$$

There, however, we shall retain only the term of zeroth order in $\gamma\tau$. That is, we shall take

$$e^{-i(\gamma_{m\beta}-\gamma^{*}_{n\beta})\tau} \simeq 1. \qquad (3.54)$$

The reason for doing so is that the factors $J^{(\pm)}(\tau)$ appear in terms which are already proportional to $|D|^2$ and we must neglect terms of order higher than the second in $|D|$, if our approximation scheme is to be consistent. We still have γ's occurring in the remaining factors of Eq. (3.52). When the summations over β and β_1 are performed, however, and the γ's are replaced by their averages, it can be argued that the γ's cancel, to a certain approximation. Note that this is rigorously so when the interaction with the perturber is switched off. Subsequently we shall indicate how the summation over β, β_1 is performed. Before doing so, we give the differential equation that one obtains after all the above-discussed approximations are made.

$$\frac{d}{dt}\rho^R_{mn}(t) = \rho^R_{mn}(t)\left[-i(m-n)\omega - i\sum_\beta \rho^B_{\beta\beta}\left(\gamma_{m\beta} - \gamma^*_{n\beta}\right)\right] +$$

$$+ \sqrt{(m+1)(n+1)}\,\rho^R_{(m+1)(n+1)}(t)\sum'_{\beta\beta_1}\rho^B_{\beta_1\beta_1}\left|D_{\beta\beta_1}\right|^2\frac{J^{(+)}_{\beta\beta_1}(\tau)}{\tau} +$$

$$+ \sqrt{mn}\,\rho^R_{(m-1)(n-1)}(t)\sum'_{\beta\beta_1}\rho^B_{\beta_1\beta_1}\left|D_{\beta\beta_1}\right|^2\frac{J^{(-)}_{\beta\beta_1}(\tau)}{\tau}\,, \qquad (3.55)$$

where the quantities $\dfrac{J^{(\pm)}(\tau)}{\tau}$ are to be interpreted as independent of τ.

It is at this point that one must either specify H^P and V^c and then solve the eigenvalue problem (3.38) to determine $|\beta\rangle$, or make suitable assumptions which will be satisfied by a rather general class of perturbing interactions. We will choose the second alternative since we are not considering a specific material. Recall that the eigenstates $|\beta\rangle$ are generated by the Hamiltonian $H^B = H^A + H^P + V^c$ where H^A is the Hamiltonian of the two-level system. If the interaction V^c is switched off, the eigenstates $|\beta\rangle$ reduce to the eigenstates of H^A because the states of H^P do not come into play any more since it does not interact with either (A) or the field mode. Then, the summations over β reduce to

summations over the two states of H^A and we obtain the results of the previous report. The density operator ρ^B will then reduce to the density operator ρ^A of the two-level system with matrix elements ρ^A_{11} and ρ^A_{22}.

Now, we know that when H^A is in weak interaction with the perturber, the levels of H^A are not sharply defined anymore. Instead, we have levels around the previous sharp levels, distributed according to a certain distribution determined by the nature of H^P and the interaction. If the interaction is not too strong, these distributions are peaked around the levels of H^A. Loosely speaking, we might say that the two-level atoms can be found to have energies around the previously sharp energy levels. Let us, therefore, assume that these distributions are characterized by the functions $\sigma_1(\omega_\beta, \omega_1)$ and $\sigma_2(\omega_\beta, \omega_2)$. These are functions of ω_β which are assumed to be very peaked, the first about ω_1, and the second about ω_2. The frequencies ω_1 and ω_2 are defined by

$$\omega_1 = \frac{E_1}{\hbar} \text{ and } \omega_2 = \frac{E_2}{\hbar} , \tag{3.56}$$

where E_1 and E_2 $(E_1 < E_2)$ are the eigenvalues of H^A. These distribution functions σ are to be used as follows: whenever we have a summation over β, we shall replace it by

$$\sum_{j=1}^{2} \int \sigma_j(\omega', \omega j)\, d\omega' \quad . \tag{3.57}$$

For example, an expression of the form

$$\sum_{\beta\beta'} \rho^B_{\beta\beta} \left|D_{\beta\beta'}\right|^2 F(\omega_\beta, \omega_{\beta'}) \tag{3.58}$$

where $F(\omega_\beta, \omega_{\beta'})$ is some function of ω_β and $\omega_{\beta'}$ will be replaced by

$$\rho^A_{11} \left|D_{12}\right|^2 \int \sigma_1(\omega_\beta, \omega_1)\sigma_2(\omega_{\beta'}, \omega_2)\, F(\omega_\beta, \omega_{\beta'})\, d\omega_\beta\, d\omega_{\beta'} +$$

$$+ \rho^A_{22} \left|D_{21}\right|^2 \int \sigma_2(\omega_\beta, \omega_2)\sigma_1(\omega_{\beta'}, \omega_1)\, F(\omega_\beta, \omega_{\beta'})\, d\omega_\beta\, d\omega_{\beta'} \quad . \tag{3.59}$$

Here, ρ_{11}^{A} and ρ_{22}^{A} are the fractional populations of the lower and upper levels and $|D_{12}|^2 = |D_{21}|^2$ the usual coupling matrix element. Now, one can make use of the peaked character of the function σ and simplify the results further. This is possible because the functions F that appear in our integrals will themselves be peaked (resonant) functions of ω_β and $\omega_{\beta'}$. Clearly, the function σ depends on the density of levels of H^P and the interaction V^C. To actually determine these functions, one has no other alternative but to solve the eigenvalue problem (3.38). Here, we shall leave them completely general except for requiring that they be peaked.

Using now the prescription (3.57), (3.58), and (3.59), we may proceed to compute the summations appearing in Eq. (3.55). This calculation is extremely lengthy and involved. We refrain from reproducing it here, and we simply give the final result. The differential equation for $\rho_{mn}^{R}(t)$ turns out to be

$$\frac{d}{dt}\rho_{mn}^{R}(t) = -i(m-n)\omega\rho_{mn}^{R}(t) -$$

$$-\left[c_2\left\{(m+1)K(\omega)+(n+1)K(\omega)\right\}+c_1\left(mK(\omega)+nK^*(\omega)\right)\right]\rho_{mn}^{R}(t) +$$

$$+ b_2\sqrt{mn}\,\rho_{(m-1)(n-1)}^{R}(t) + b_1\sqrt{(m+1)(n+1)}\,\rho_{(m+1)(n+1)}^{R}(t)\,, \qquad (3.60)$$

where

$$c_j = \rho_{jj}^{A} d^2 h^{-2}\,, \qquad j = 1, 2, \qquad (3.61)$$

$$b_j = 2\pi c_j g(\omega, \omega_o) = 2\pi\hbar^{-2}\rho_{jj}^{A} d^2 g(\omega, \omega_o)\,, \qquad (3.62)$$

$$K(\omega) = \pi g(\omega, \omega_o) + i f(\omega, \omega_o)\,, \qquad (3.63)$$

$$\omega_o = \frac{E_2 - E_1}{\hbar}\,, \qquad (3.64)$$

and the functions $g(\omega, \omega_o)$, $f(\omega, \omega_o)$ are given by

$$g(\omega, \omega_o) = \int \sigma_1(\omega', \omega_1)\sigma_2(\omega+\omega', \omega_2)\, d\omega' \tag{3.65}$$

and

$$f(\omega, \omega_o) = P \int\int \frac{\sigma_1(\omega', \omega_1)\sigma_2(\omega'', \omega_2)}{\omega' + \omega - \omega''}\, d\omega'\, d\omega'' . \tag{3.66}$$

The form of Eq. (3.60) is identical to that of the analogous equation we had found in the previous Interim Report. The important thing, however, is that the coefficients b_1, b_2 and K now do not contain δ-functions but the line shape functions $g(\omega)$ and $f(\omega)$. In fact, we have expressed these functions in terms of the functions σ_1 and σ_2, as is seen from Eqs. (3.65) and (3.66). Note that if we take $\sigma_1(\omega', \omega_1) = \delta(\omega' - \omega_1)$ and $\sigma_2(\omega', \omega_2) = \delta(\omega' - \omega_2)$ we shall obtain

$$g(\omega, \omega_o) = \delta(\omega - \omega_o) , \tag{3.67}$$

and

$$f(\omega, \omega_o) = \frac{P}{\omega - \omega_o} \tag{3.68}$$

and all results will reduce to those of the previous report. Of course, this is to be expected since taking σ_1 and σ_2 to be δ-functions implies that the levels of H^A are sharply defined. It is also to be noted that Eq. (3.66) does not have the unpleasant feature of becoming infinite at $\omega = \omega_o$. From the peaked character of $\sigma_1(\omega', \omega_1)$ and $\sigma_2(\omega'\omega_2)$ follows that both $g(\omega, \omega_o)$ and $f(\omega, \omega_o)$ are peaked about $\omega_o = \omega_2 - \omega_1$, as can be easily verified from Eqs. (3.65) and (3.66). Nevertheless, $f(\omega, \omega_o)$ remains finite at $\omega = \omega_o$ provided σ_1 and σ_2 are smooth functions, which is the case in practical problems. Moreover, one can easily convince himself that $g(\omega, \omega_o)$ is to be identified to the spectrum of spontaneous emission from the upper level of H^A to the lower. Thus, we now have an equation which describes the interaction of a field mode having frequency ω with a two-level system whose levels differ by ω_o when they are unperturbed. The effect of broadening is described by the functions $g(\omega)$ and $f(\omega)$. The amplifier then has a finite bandwidth and in the following section we study the gain selectivity of such an amplifier.

Up to this point we have left V^c and H^P unspecified. If we want to account for natural and collision broadening H^P should include the Hamiltonian of the whole radiation field and the Hamiltonian of the system with which the active material interacts through collisions. Similarly, V^c should include the corresponding interactions. Finally, in order to account for Doppler broadening, one should separate the Hamiltonian of the center of mass motion of the active material and include it in H^P.

3.5.3 Gain Selectivity of a Laser Preamplifier

Let now $f(\omega, 0)$ be the number of photons of frequency ω at the input of the preamplifier. Note that, in the previous report, the same quantity was denoted by $\langle f \rangle$. Here, we shall drop the angular brackets for the sake of simplicity. We have found that after amplification, the number of photons at the output is given by

$$f(\omega, t') = G(\omega, t)\, f(\omega, 0) + \big(G(\omega, t) - 1\big)\lambda \,, \tag{3.69}$$

where

$$G(\omega, t) = e^{2k(\omega)t} \,, \tag{3.70}$$

$$k(\omega) = \frac{b_2(\omega) - b_1(\omega)}{2} \,, \tag{3.71}$$

and

$$\lambda = \frac{\rho_{22}^A}{\rho_{22}^A - \rho_{11}^A} \,. \tag{3.72}$$

Note that the quantity λ is a dimensionless number which depends on the population inversion but not on frequency. Eq. (3.69) is identical to the analogous equation of the previous report except for one important difference. The quantities $k(\omega)$ and $G(\omega)$ do not contain δ-functions any more but are peaked functions of ω.

Now let us consider the following problem: A signal with power spectral density $f_{is}(\omega)$ enters the input of the amplifier. Noise with power spectral density $f_{in}(\omega)$ accompanies the signal. The number of photons at the output will be detected by a photodetector which is assumed to have a bandwidth $\Delta\omega$. Its

efficiency will be taken to be unity over the whole bandwidth $\Delta\omega$. For frequencies of the order of 10^{15} cps and bandwidths even up to 10^{12} cps, this is not a bad assumption. We would then like to compare the signal to noise ratio at the input with the signal to noise ratio at the output.

The signal power spectral density $f_{is}(\omega)$ is assumed to be appreciable only inside a certain bandwidth $\delta\omega$ and negligible otherwise. The width $\delta\omega$ is assumed to be smaller than $\Delta\omega$. One can easily convince himself that if this were not the case, the preamplifier would deteriorate the signal to noise ratio. In calculating the noise power, we shall include external noise, quantum noise (zero point fluctuations), and amplifier noise (spontaneous emission).

Let us consider the input conditions first. The total signal power at the input is:

$$S_i = \int_{\omega_o - \frac{\delta\omega}{2}}^{\omega_o + \frac{\delta\omega}{2}} f_{is}(\omega)d\omega, \tag{3.73}$$

where ω_o denotes the carrier frequency which will be assumed to coincide with the transition frequency of the two-level system of the laser material. As we have discussed in previous reports, the zero-point fluctuations add one quantum of noise per unit bandwidth. Consequently, the noise per unit bandwidth at the input will be $f_{in}(\omega)+1$. The total noise at the input will be

$$N_i = \int_{\omega_o - \frac{\Delta\omega}{2}}^{\omega_o + \frac{\Delta\omega}{2}} \left(f_{in}(\omega)+1\right)d\omega \quad . \tag{3.74}$$

The incident noise f_{in} will presumably be thermal noise. For the frequency range and bandwidths of interest in this contract, we may assume that f_{in} is constant to a very good approximation. Under this assumption, Eq. (3.74) gives

$$N_i = (f_{in} + 1)\,\Delta\omega\,. \tag{3.75}$$

If we denote by r_i the signal to noise ratio at the input, we shall have

$$r_i = \frac{S_i}{N_i} = \frac{\int_{\omega_o - \frac{\delta\omega}{2}}^{\omega_o + \frac{\delta\omega}{2}} f_{is}(\omega)d\omega}{(f_{in} + 1)\,\Delta\omega} . \tag{3.76}$$

We now turn to the output conditions. From Eq. (3.69) we find that the number of photons per unit bandwidth at the output will be

$$f_o(\omega, t) = G(\omega)\left(f_{is}(\omega) + f_{in}\right) + \left(G(\omega) - 1\right)\lambda \quad . \tag{3.77}$$

This, however, contains the amplified external noise as well as the spontaneous emission noise. The first is given by $G(\omega) f_{in}$, while the second is given by $(G-1)\lambda$. Thus if we denote by $f_{os}(\omega)$ the signal and by $f_{on}(\omega)$ the noise power spectral densities at the output, we shall have

$$f_{os}(\omega) = G(\omega) f_{is}(\omega) \tag{3.78}$$

and

$$f_{on}(\omega) = G(\omega) f_{in} + \left(G(\omega) - 1\right)\lambda + 1 \tag{3.79}$$

where we have also added the noise due to the zero-point fluctuations. As has been noted by several authors, this quantum noise can be thought of as remaining unaffected by the amplification process. Of course, this is only a pictorial way of speaking since the zero-point fluctuations have to do with the uncertainty principle. Now, the total output signal and noise will be, respectively,

$$S_o = \int_{\omega_o - \frac{\delta\omega}{2}}^{\omega_o + \frac{\delta\omega}{2}} f_{os}(\omega)d\omega = \int_{\omega_o - \frac{\delta\omega}{2}}^{\omega_o + \frac{\delta\omega}{2}} G(\omega) f_{is}(\omega)d\omega , \tag{3.80}$$

and

$$N_o = \int_{\omega_o - \frac{\Delta\omega}{2}}^{\omega_o + \frac{\Delta\omega}{2}} f_{os}(\omega)d\omega = \int_{\omega_o - \frac{\Delta\omega}{2}}^{\omega_o + \frac{\Delta\omega}{2}} \left[G(\omega) f_{in} + (G(\omega) - 1)\lambda + 1 \right] d\omega . \qquad (3.81)$$

Then, if we denote by r_o the signal to noise ratio after amplification we shall have

$$r_o = \frac{S_o}{N_o} = \frac{\int_{\omega_o - \frac{\delta\omega}{2}}^{\omega_o + \frac{\delta\omega}{2}} G(\omega) f_{is}(\omega)d\omega}{\int_{\omega_o - \frac{\Delta\omega}{2}}^{\omega_o + \frac{\Delta\omega}{2}} \left[G(\omega) f_{in} + (G(\omega) - 1)\lambda + 1 \right] d\omega} \qquad (3.82)$$

Let us denote by R the ratio of the two signal to noise ratios. That is,

$$R = \frac{r_o}{r_i} . \qquad (3.83)$$

Now, we shall investigate the conditions under which R is greater than unity in which case the preamplifier improves the signal to noise ratio.

We have already assumed that the signal power spectral density $f_{is}(\omega)$ is appreciable only inside a bandwidth $\delta\omega$. Let us also assume that the amplifier is chosen such that its gain is unity outside the band $\delta\omega$. Then, we define the average gain G given by

$$\bar{G} = \frac{1}{\delta\omega} \int_{\omega_o - \frac{\delta\omega}{2}}^{\omega_o + \frac{\delta\omega}{2}} G(\omega)d\omega . \qquad (3.84)$$

Recalling that f_{in} is constant inside the bandwidths of interest, and after some straightforward manipulation we find

$$N_o = (\bar{G}-1)(f_{in}+\lambda)\,\delta\omega + (f_{in}+1)\,\Delta\omega \,. \tag{3.85}$$

Now let us define an effective gain G_e given by

$$G_e = \frac{\int_{\omega_o-\frac{\delta\omega}{2}}^{\omega_o+\frac{\delta\omega}{2}} G(\omega) f_{is}(\omega)\,d\omega}{\int_{\omega_o-\frac{\delta\omega}{2}}^{\omega_o+\frac{\delta\omega}{2}} f_{is}(\omega)\,d\omega} \,. \tag{3.86}$$

Then, we have

$$S_o = G_e \int_{\omega_o-\frac{\delta\omega}{2}}^{\omega_o+\frac{\delta\omega}{2}} f_{is}(\omega)\,d\omega \,. \tag{3.87}$$

Using (3.83), (3.85) and (3.87) we obtain

$$R = \frac{G_e}{(\bar{G}-1)\left(\frac{f_{in}+\lambda}{f_{in}+1}\right)\left(\frac{\delta\omega}{\Delta\omega}\right)+1} \tag{3.88}$$

Let us, finally, define ζ by

$$\zeta = \left(\frac{f_{in}+\lambda}{f_{in}+1}\right)\left(\frac{\delta\omega}{\Delta\omega}\right) \,. \tag{3.89}$$

Then (3.88) becomes

$$R = \frac{G_e}{(\bar{G}-1)\zeta+1} \tag{3.90}$$

Let us first investigate the order of magnitude of ζ. Since the external noise

is assumed to be thermal noise we shall have

$$f_{in} = \frac{kT}{\hbar\omega_o} \quad . \tag{3.91}$$

For the frequencies of interest to us and usual noise temperatures, we shall have either $f_{in} \simeq 1$ or $f_{in} < 1$. As we have discussed in the previous report, for almost any practical active material we would have $\lambda < 10$. Therefore, the order of magnitude of ζ will be determined primarily by the order of magnitude of $\frac{\delta\omega}{\Delta\omega}$. The bandwidth $\Delta\omega$ depends on the photodetector while $\delta\omega$ will depend on the amplifier. The latter could probably be as low as 50 Mcps, for solid state laser amplifiers. As for $\Delta\omega$, one would expect it to be at least four orders of magnitude larger than $\delta\omega$. Thus, a rough estimate of ζ would be from 10^{-1} to 10^{-4}. Of course, these limits are not intended to represent precise upper and lower bounds but rather typical values of ζ. It is evident now that the magnitude of R will depend substantially on the relative magnitudes of G_e and $\bar{G}$. Since G_e depends on the spectral shape $f_{in}(\omega)$ of the signal, so does R. There is a special case, however, in which R is independent of the spectral shape of the signal. This happens when $G(\omega)$ has a square form and is the subject of the following section.

3.5.4 Results for a Special Case

Let us assume now that $G(\omega)$ is given by

$$G(\omega) = G_o \text{ for } \omega_o - \frac{\delta\omega}{2} < \omega < \omega_o + \frac{\delta\omega}{2} \tag{3.92}$$

$$= 1 \text{ otherwise.}$$

Then, from Eqs.(3.84) and (3.86) we obtain

$$\bar{G} = G_e = G_o \quad , \tag{3.93}$$

and consequently

$$R = \frac{G_o}{(G_o - 1)\zeta + 1} \quad . \tag{3.94}$$

If, in addition, ζ is such that $G_o \zeta << 1$, we shall have

$$R \cong G_o . \tag{3.96}$$

For gain $G_o = 10$, for example, we have an improvement of 10 dbs.

In the general case in which the conditions $G_o >> 1$ and $G_o \zeta << 1$ are not necessarily satisfied, one should investigate the behavior of R as a function of G_o and ζ. The results of this investigation are given in Fig. 18 where we have plotted R as a function of G_o for three values of the parameter ζ. From this figure, it is evident that, for a given ζ, R increases rather fast as the gain increases up to a certain point. Further increase of the gain does not give any substantial improvement. One also sees that improvement of the order of 10 db can be obtained with a rather low gain (approximately $G_o = 10$) as long as ζ is smaller than 10^{-2}. Values of ζ much smaller than 10^{-2} should be easily achievable so that one could have 20 db improvement with gain approximately 100.

Before closing this section, a comment should be made as to the actual shape of $G(\omega)$. Recall that

$$G(\omega) = e^{Bk(\omega)} . \tag{3.97}$$

In most practical cases, the shape of $k(\omega)$ can be approximated by a Lorentzian, i.e.

$$k(\omega) \sim \frac{\gamma}{(\omega-\omega_o)^2 + \gamma^2} , \tag{3.98}$$

where B and γ are constants. Then $G(\omega)$ will be the exponential of the Lorentzian. In Fig. 19 we have plotted $k(\omega)$ normalized to unity. We have also plotted $G(\omega)$ for maximum gain 20 and 150, again normalized to unity. As is seen from the figure, considerable narrowing and hence selectivity results because of the exponential form of $G(\omega)$. That is, the selectivity of the material is enhanced as the gain is increased. It should also be born in mind that additional selectivity results if the signal itself is a function of ω peaked around ω_o.

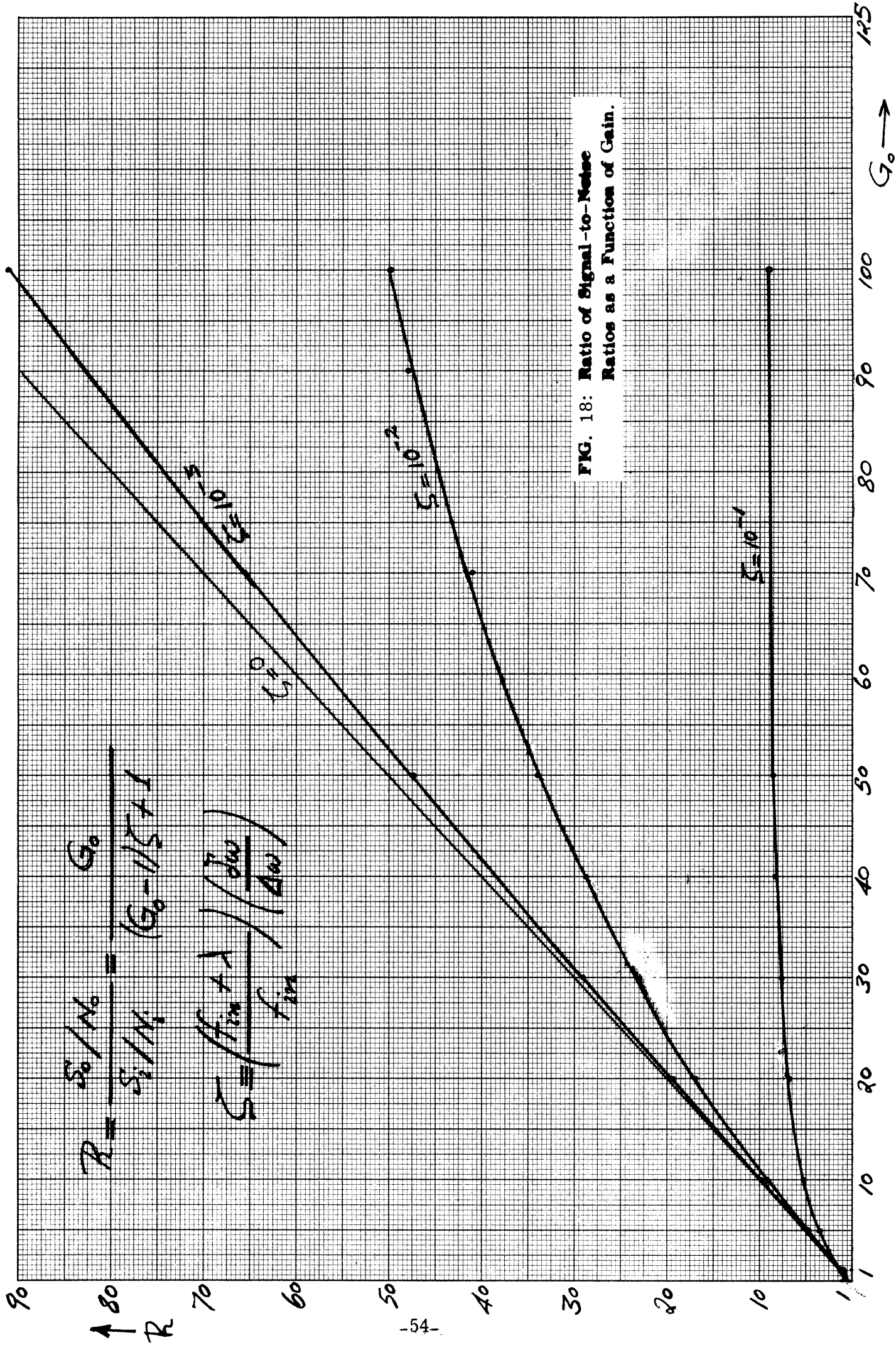

FIG. 18: Ratio of Signal-to-Noise Ratios as a Function of Gain.

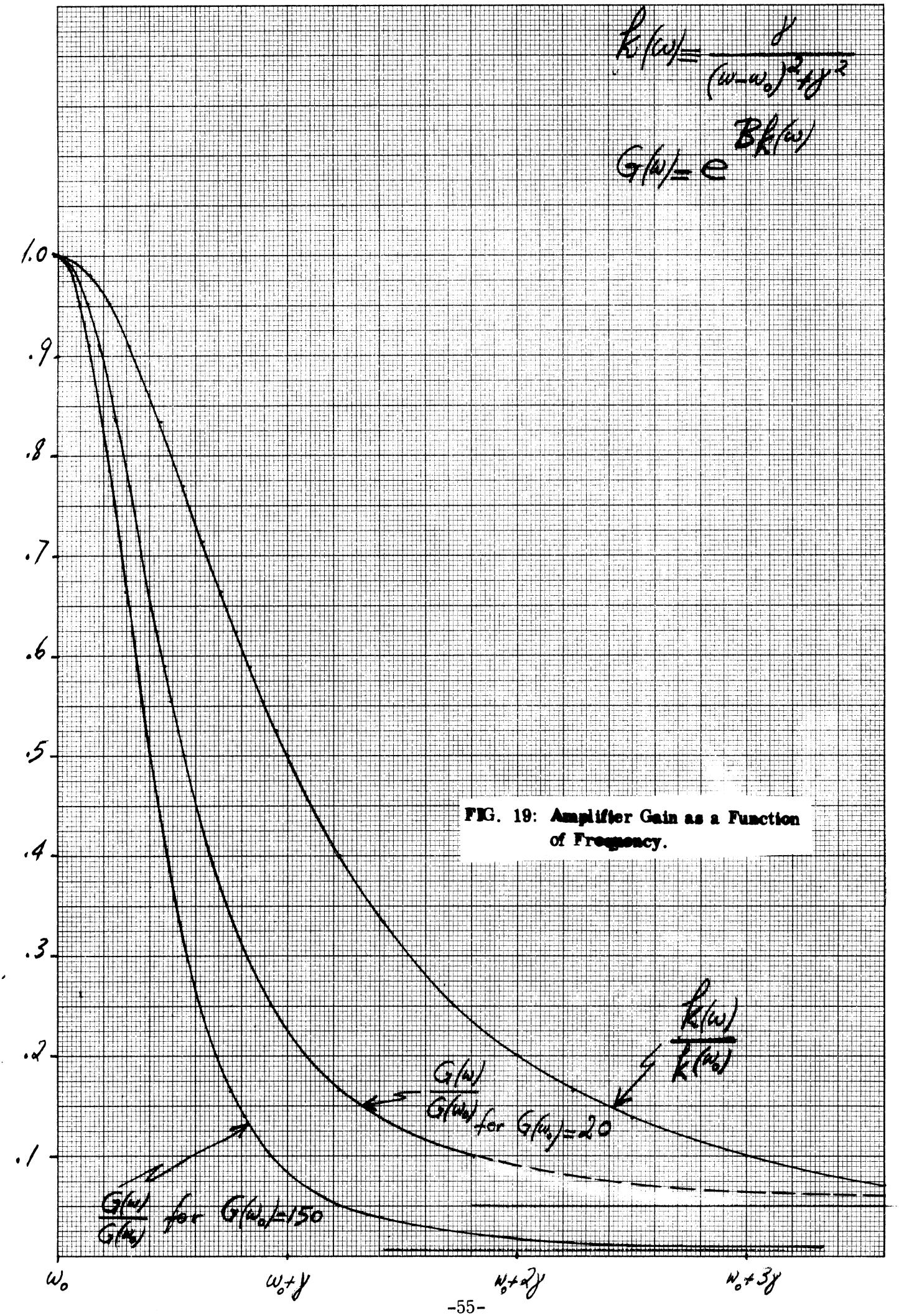

FIG. 19: Amplifier Gain as a Function of Frequency.

3.5.5 Solution of the Equation for the Density Operator of a Mode of the Electromagnetic Field Amplified by a Quantum Amplifier

In a previous study (Interim Report 06515-4-T), we found that the matrix elements of the density operator ρ^R of a field mode passing through a quantum amplifier obey the differential equation

$$\dot{\rho}_{(m+\ell)m}(t) = -(bm+c)\rho_{(m+\ell)m}(t) + b_2\sqrt{(m+\ell)m}\;\rho_{(m+\ell-1)(m-1)}(t) + b_1\sqrt{(m+\ell+1)(m+1)}\;\rho_{(m+\ell+1)(m+1)}(t), \tag{3.99}$$

where the superscript R has been dropped and the matrix elements are calculated in the photon number representation. The quantities b, b_1, b_2 and c are known constants depending on the parameter of the amplifier. Let it be mentioned that, although one can calculate average values and fluctuations of operators without knowing the solution of Eq. (3.99), knowledge of the solution will be necessary in order to calculate probability distributions of the values of pertinent operators. Such probability distributions are needed in calculating, for example, the rate of false alarms, misses, etc. The solution of Eq. (3.99), therefore, is not a matter of pure academic interest.

For $\ell = 0$, we obtain the subset of the diagonal matrix elements of ρ. The corresponding set of differential equations (for $m=0, 1, 2\cdots$) has been solved by Shimoda et al (1957), by means of an appropriate generating function. For $\ell \neq 0$ the form of the equations is different (because of the presence of the square roots) and does not lend itself to direct use of the techniques of Shimoda et al. At this point, we observe that if we introduce a new set of functions $F_{mn}(t)$ defined by

$$F_{mn}(t) = \rho_{mn}(t)\sqrt{\frac{m!}{n!}}, \tag{3.100}$$

and substitute into Eq.

$$\dot{F}_m^{(\ell)}(t) = -(bm+c)F_m^{(\ell)}(t) + b_2(m+\ell)F_{m-1}^{(\ell)}(t) + b_1(m+1)F_{m+1}^{(\ell)}(t) \tag{3.101}$$

where we have changed the notation slightly. That is, we have written $F_m^{(\ell)}$ instead of $F_{(m+\ell)m}(t)$. Thus, we have a family of sets of differential equations parametrized by ℓ, where $\ell=0,1,2\cdots$. From Eq. (3.100) we have

$$\rho_{(m+\ell)m}(t) = F_m^{(\ell)}(t)\sqrt{\frac{m!}{(m+\ell)!}} \quad . \tag{3.102}$$

The problem has now been reduced to solving the equation for $F_m^{(\ell)}(t)$. The advantage of the transformation (3.100) is that the resulting equation for $F_m^{(\ell)}(t)$ is similar to the equation obtained from (3.99) by setting $\ell=0$, and can therefore be solved by using the techniques of Shimoda et al (1957).

To this end, we introduce a generating function $R^{(\ell)}(X,t)$ defined by

$$R^{(\ell)}(X,t) = \sum_{m=0}^{\infty} F_m^{(\ell)}(t)\, X^m. \tag{3.103}$$

We have a family of generating functions parametrized by ℓ. Again, for $\ell=0$ we obtain the generating function of Shimoda et al (1957). Taking the partial derivative of $R^{(\ell)}$ with respect to time, and using Eq. (3.101)

$$\frac{\partial R}{\partial t} + (1-X)(b_2X-b_1)\frac{\partial R}{\partial X} + (c-aX)R = 0, \tag{3.104}$$

where we have introduced

$$a = b_2(\ell+1). \tag{3.105}$$

The superscript ℓ has been dropped from Eq. (3.104) for the sake of simplicity. The dependence of R on the parameter ℓ is implicit in the coefficients a and c. Note that for $\ell=0$, we have $a=c=b_2$. The task now is to solve the partial differential (3.104) and express the solution as a series in powers of X. Of course, the initial condition will be a given set of matrix elements $\rho_{mn}(0)$ and hence a known set of numbers $F_m^{(\ell)}(0)$.

To solve Eq. (3.104), we consider the equivalent system of ordinary differential equations

$$\frac{dX}{(1-X)(b_2X-b_1)} = dt = \frac{dR}{(aX-c)R} . \tag{3.106}$$

Introducing

$$y = \frac{1}{1-X} , \tag{3.107}$$

the first equation gives

$$\frac{dy}{dt} = 2ky - b_2 \tag{3.108}$$

where k stands for the quantity $\frac{b_2 - b_1}{2}$, as in Interim Report 06515-4-T. The solution of Eq. (3.108)

$$y(t) = y_o e^{2kt} + \lambda \tag{3.109}$$

where

$$\lambda = \frac{b_2}{2k} = \frac{b_2}{b_2 - b_1} \tag{3.110}$$

Considering now the second differential equation and using the above expression for y(t), one can solve for R. The result is

$$R(X,t) = C\, e^{-i\nu\ell t} e^{\ell kt} (\lambda e^{-2kt} + y_o)^{\ell+1} , \tag{3.111}$$

where C is the constant of integration.

Let now $\rho(0)$ be the density operator of the field mode at t=0. Then, its matrix elements will be $\rho_{mn}(0)$ and from Eq. (3.102) we have

$$F_m^{(\ell)}(0) = \sqrt{\frac{(m+\ell)!}{m!}}\, \rho_{(m+\ell)m}(0) . \tag{3.112}$$

Thus, the initial value of R(x,t) is

$$R_o = \sum_{m=0}^{\infty} F_m^{(\ell)}(0)\, X_o^m . \tag{3.113}$$

Now, setting t=0 in Eq. (3.111) and using Eq. (3.113), we find

$$C = (y_o+\lambda)^{-(\ell+1)} \sum_{m=0}^{\infty} F_m^{(\ell)}(0)\, X_o^m \,. \tag{3.114}$$

This equation determines the constant of integration. Substituting into Eq. (3.111), we obtain

$$R(x,t) = \left(\sum_{m=0}^{\infty} F_m^{(\ell)}(0)\, X_o^m\right) e^{\ell(k-i\nu)t} \left(\frac{y_o+\lambda e^{-2kt}}{y_o+\lambda}\right)^{\ell+1} \tag{3.115}$$

Now introduce the quantity

$$G = e^{2kt}, \tag{3.116}$$

as defined in Interim Report 06515-4-T. Then, from Eq. (3.109) we have

$$y = y_o G + \lambda, \tag{3.117}$$

from which we obtain

$$y_o = \frac{1}{G}(y-\lambda). \tag{3.118}$$

Using this relation and the fact that

$$X_o = 1 - \frac{1}{y_o}, \tag{3.119}$$

we find

$$X_o = \frac{y-(\lambda+G)}{y-\lambda}. \tag{3.120}$$

Recalling the definition of y (see Eq. (3.107), we obtain

$$X_o = \frac{1-(\lambda+G)(1-X)}{1-\lambda(1-X)}. \tag{3.121}$$

Similarly, using Eqs. (3.116), (3.117), and (3.107), we find

$$\frac{y_o + \lambda e^{-2kt}}{y_o + \lambda} = \frac{1}{1 + \lambda(G-1)(1-X)} . \tag{3.122}$$

It will be more convenient to write Eqs. (3.121) and (3.122) as follows:

$$X_o = \frac{G+\lambda-1}{\lambda-1} \frac{1 - \frac{G+\lambda}{G+\lambda-1} X}{1 - \frac{\lambda}{\lambda-1} X} , \tag{3.123}$$

and

$$\frac{y_o + \lambda e^{-2kt}}{y_o + \lambda} = \frac{1}{1 + \lambda(G-1)} \frac{1}{1 - \frac{\lambda(G-1)}{1+\lambda(G-1)} X} . \tag{3.124}$$

Now, for the sake of simplicity, introduce the parameters

$$\xi = \frac{G+\lambda-1}{\lambda-1} , \tag{3.125a}$$

$$\eta = \frac{G+\lambda}{G+\lambda-1} , \tag{3.125b}$$

$$\mu = \frac{1}{1+\lambda(G-1)} . \tag{3.125c}$$

Also, note that $\frac{\lambda}{\lambda-1} = \frac{b_2}{b_1}$ where we have used Eq. (3.110). Finally, introduce the parameter

$$z = \frac{\lambda(G-1)}{1 + \lambda(G-1)} . \tag{3.126}$$

Comparing this to Eq. (3.125c) one finds

$$z = \mu \lambda(G-1) . \tag{3.127}$$

Using now Eqs. (3.125) and (3.126), we obtain

$$X_o = \frac{1 - \eta X}{1 - \frac{b_2}{b_1} X}, \tag{3.128a}$$

and

$$\frac{y_o + \lambda e^{-2kt}}{y_o + \lambda} = \frac{\mu}{1 - zX}. \tag{3.128b}$$

Substituting into Eq. (3.115) we have

$$R(X,t) = e^{\ell(k-i\nu)t} \sum_{m=0}^{\infty} F_m^{(\ell)}(0) \xi^m (1-\eta X)^m \left(1 - \frac{b_2}{b_1} X\right)^{-m} \frac{\mu^{\ell+1}}{(1-zX)^{\ell+1}}. \tag{3.129}$$

Using the identities

$$(1-\alpha)^{-n} = \sum_{r=0}^{\infty} (-1)^r \frac{n!}{r!\,(n-r)!} \alpha^r, \tag{3.130a}$$

$$(1-\alpha)^{-n} = \sum_{q=0}^{\infty} \frac{(n-1+q)!}{(n-1)!\,q!} \alpha^q, \tag{3.130b}$$

Eq. (3.129) becomes

$$R(X,t) = \mu^{\ell+1} e^{\ell(k-i\nu)t} \sum_{m=0}^{\infty} \sum_{r=0}^{\infty} \sum_{j=0}^{\infty} \sum_{q=0}^{\infty} (-1)^r F_m^{(\ell)}(0) \xi^m \eta^r \left(\frac{b_2}{b_1}\right)^j z^q \frac{m!(m-1+j)!\,(\ell+q)!}{r!(m-r)!(m-1)!j!\ell!q!} X^{r+j+q}. \tag{3.131}$$

Making now the substitution

$$r + j + q = M, \tag{3.132}$$

$$R(X,t) = \mu^{\ell+1} e^{\ell(k-i\nu)t}$$

$$\sum_{j=0}^{\infty}\sum_{q=0}^{\infty}\sum_{m=0}^{\infty}\sum_{M=j+q}^{m+j+q} (-1)^{M-j-q} F_m^{(\ell)}(0)\,\xi^m \eta^{M-j-q}\left(\frac{b_2}{b_1}\right)^j$$

$$z^q \frac{m!(m-1+j)!(\ell+q)!}{(M-j-q)!(m-M+j+q)!(m-1)!j!\ell!q!} X^M. \qquad (3.133)$$

Comparing this to Eq. (3.103), that is considering a specific M, and using Eq. (3.102), we obtain the final result

$$\rho_{(M+\ell)M}(t) = (-\eta)^M \sqrt{\frac{M!}{(M+\ell)!}}\,\mu^{\ell+1} e^{\ell(k-i\nu)t} \sum_{m=0}^{\infty}\sum_{j=0}^{\infty}\sum_{q=0}^{\infty} \rho_{(m+\ell)m}(0)\,\xi^m (-1)^{j+q}\left(\frac{b_2}{\eta b_1}\right)^j \left(\frac{z}{\eta}\right)^q$$

$$\frac{\sqrt{(m+\ell)!\,m!}}{(m-1)!\,\ell!}\,\frac{(m-1+j)!}{(M-j-q)!}\,\frac{(\ell+q)!}{(m+j+q-M)!\,j!\,q!}, \qquad (3.134)$$

or in a slightly different from

$$\rho_{(M+\ell)M}(t) = (-\eta)^M \sqrt{\frac{M!}{(M+\ell)!}}\,\mu^{\ell+1} e^{\ell(k-i\nu)t} \sum_{m=0}^{\infty} \rho_{(m+\ell)m}(0)\,\xi^m \frac{\sqrt{(m+\ell)!\,m!}}{(m-1)!\,\ell!}$$

$$\sum_{j=0}^{\infty}\sum_{q=0}^{\infty} (-1)^{j+q}\left(\frac{b_2}{\eta b_1}\right)^j \left(\frac{z}{\eta}\right)^q \frac{(m-1+j)!\,(\ell+q)!}{(M-j-q)!\,(m+j+q-M)!\,j!\,q!}. \qquad (3.135)$$

Although the summations extend formally from zero to infinity, in fact they are limited by the requirement that none of the factorials be negative. This restriction stems from the initial Eq. (3.131)

Letting $\ell = 0$ in Eq. (3.135), we obtain the solution for the diagonal matrix elements, that is,

$$\rho_{MM}(t) = (-\eta)^{M}\mu \sum_{m=0}^{\infty} \rho_{mm}(0)\xi^{m} \frac{m!}{(m-1)!} \sum_{j=0}^{\infty}\sum_{q=0}^{\infty} (-1)^{j+q} \left(\frac{b_2}{\eta b_1}\right)^{j} \left(\frac{z}{\eta}\right)^{q} \frac{(\quad+j+q)!}{(M-j-\quad)!\,(\quad+j)!\,(\quad-M)!\,j!}$$

(3.136)

This, however, is not Shimoda et al's (1957) result yet. These authors assume that the field mode in the initial state has a precise number of photons. This means that

$$\rho_{mm}(0) = \delta_{mm_o}, \tag{3.137}$$

where m_o is the initial number of photons. Therefore, by deleting the summation over m in Eq. (3.136) and replacing m by m_o, we obtain a result equivalent to that of Shimoda et al (1957). Note that all parameters appearing in Eqs. (3.135) and (3.136) depend on the two parameters G(gain) and λ (population inversion) of the amplifier.

IV. BIBLIOGRAPHY

Akcasu, A. Z., (1963) "A Study of Line Shape with Heitler's Damping Theory," University of Michigan Technical Report 04836-1-T, April 1963.

Barasch, M. L., G. Hok, P. Lambropoulos and E. K. Miller, (1964) "Study of Problem Areas in Optical Communications," First Interim Report, University of Michigan Radiation Laboratory Report No. 06515-1-T, 31 July 1964.

Elterman, L., (1963) "A Model of a Clear Standard Atmosphere for Attenuation in the Visible Region and Infrared Windows," Report No. AFCRL-63-675, July 1963.

Gaertner, H., (1957) "The Transmission of Infrared in a Cloudy Atmosphere," NAVORD Report No. 429, U. S. Government Printing Office, Washington, D. C.

Goldberg, L., (1934) "The Absorption Spectrum of the Atmosphere, The Solar System, Vol. II, The Earth as a Planet, Chapter IX, Ed. G. Kuiper, University of Chicago Press.

Gordon, J. P. (1962) "Quantum Effects in Communications Systems," Proc. IRE, 50, 1898.

Hok, G., M. L. Barasch, P. Lambropoulos and E. K. Miller, (1964) "Study of Problem Areas in Optical Communications," Second Interim Report, University of Michigan Radiation Laboratory Report 06515-2-T, 31 October 1964.

Hok, G., M. L. Barasch, P. Lambropoulos and E. K. Miller, (1965) "Study of Problem Areas in Optical Communications," Third Interim Report, University of Michigan Radiation Laboratory Report 06515-3-T, January 1965.

Hok, G., M. L. Barasch, P. Lambropoulos and E. K. Miller, (1965) "Study of Problem Areas in Optical Communications," Fourth Interim Report, University of Michigan Radiation Laboratory Report 06515-4-T, April 1965.

Howard, J. N. and J. S. Garing, (1962) "Transmission of the Atmosphere in the Infrared - A Review," Air Force Surveys in Geophysics, No. 150, AFCRL, July 1962.

Messiah, A., (1964) Mecanique Quantique, Tome II, Dunod, Paris.

Plass, G. N. (1963) "Infrared Transmission Studies, Final Report - Vol. V: Transmittance Tables for Slant Paths in the Stratosphere," Aeronutronic Division, Ford Motor Company, Newport Beach, Cal.

Shimoda, K., H. Takahashi and C. H. Townes, (1957) "Fluctuations in Amplification of Quanta with Application to Maser Amplifiers," J. Phys. Soc. Japan, 12, pp. 686-700.

Slepian, D. (1965) "Permutation Modulation," Proc. IEEE, 53, p. 228, March 1965.